Annu. Rev. Phys. Chem. 2004. 55:427–55
doi: 10.1146/annurev.physchem.55.091602.094449

First published online as a Review in Advance on January 27, 2004

# TIME-DEPENDENT DENSITY FUNCTIONAL THEORY

M.A.L. Marques and E.K.U. Gross
*Institut für Theoretische Physik, Freie Universität Berlin, Arnimallee 14, D-14195 Berlin, Germany; email: marques@tddft.org, hardy@physik.fu-berlin.de*



**Key Words** exchange-correlation functionals, linear response theory, optical absorption spectra, strong lasers

■ **Abstract** Time-dependent density functional theory (TDDFT) can be viewed as an exact reformulation of time-dependent quantum mechanics, where the fundamental variable is no longer the many-body wave function but the density. This time-dependent density is determined by solving an auxiliary set of noninteracting Schrödinger equations, the Kohn-Sham equations. The nontrivial part of the many-body interaction is contained in the so-called exchange-correlation potential, for which reasonably good approximations exist. Within TDDFT two regimes can be distinguished: (*a*) If the external time-dependent potential is "small," the complete numerical solution of the time-dependent Kohn-Sham equations can be avoided by the use of linear response theory. This is the case, e.g., for the calculation of photoabsorption spectra. (*b*) For a "strong" external potential, a full solution of the time-dependent Kohn-Sham equations is in order. This situation is encountered, for instance, when matter interacts with intense laser fields. In this review we give an overview of TDDFT from its theoretical foundations to several applications both in the linear and in the nonlinear regime.

## INTRODUCTION

It was in 1964 that Hohenberg & Kohn (1) discovered that to fully describe a stationary electronic system it is sufficient to know its ground-state density. From this quantity all observables (and even the many-body wave function) can, in principle, be obtained. The density is a very convenient variable: it is a physical observable, it has an intuitive interpretation, and it depends only on three spatial coordinates, in contrast to the many-body wave function, which is a complex function of $3N$ spatial coordinates. Hohenberg & Kohn also established a variational principle in terms of the density by showing that the total energy can be written as a density functional whose minimum, the exact ground-state energy of the system, is attained at the exact density. In this way, they put on a sound mathematical basis earlier work by Thomas (2), Fermi (3, 4), and others, who had tried to write the total energy of an interacting electron system as an explicit functional of the density.

Another breakthrough occurred when Kohn & Sham (5) proposed the use of an auxiliary noninteracting system, the Kohn-Sham system, to evaluate the density of the interacting system. Within the Kohn-Sham system, the electrons obey a simple, one-particle, Schrödinger equation with an effective external potential, $v_{\rm KS}$. As $v_{\rm KS}$ is a functional of the electronic density, the solution of this equation has to be performed self-consistently. The effective potential, $v_{\rm KS}$, is usually decomposed in the form

$$v_{\rm KS}(\boldsymbol{r}) = v_{\rm ext}(\boldsymbol{r}) + v_{\rm Hartree}(\boldsymbol{r}) + v_{\rm xc}(\boldsymbol{r}). \quad (1)$$

The first term is the external potential (normally the Coulomb interaction between the electrons and the nuclei), whereas the second includes the classical (Hartree) part of the electron-electron interaction. All the complex many-body effects are contained in the (unknown) exchange-correlation (xc) potential $v_{\rm xc}$. Kohn & Sham (5) also proposed a simple approximation to $v_{\rm xc}$, the local density approximation (LDA). This functional, that uses the knowledge of the xc energy of the homogeneous electron gas (6), turned out to be quite accurate for a number of applications, and is still widely used, especially in solid-state physics.

The use of the density as the fundamental variable, and the construction of the Kohn-Sham system form the basis of what became known as density functional theory (DFT) (7–9). The original formulation assumed an electronic system at zero temperature with a nondegenerate ground state, but has been extended over the years to encompass systems at finite temperature (10), superconductors (11, 12), relativity (13, 14), etc. An extension of somewhat different nature is time-dependent DFT (TDDFT) (15–20). The foundation of modern TDDFT was laid in 1984 by Runge & Gross (21), who derived a Hohenberg-Kohn–like theorem for the time-dependent Schrödinger equation. The scope of this generalization of DFT included the calculation of photoabsorption spectra or, more generally, the interaction of electromagnetic fields with matter, as well as the time-dependent description of scattering experiments (which was actually the original motivation of Runge and Gross). Again, the rigorous theorems of Runge and Gross put on a firm basis previous work by Ando (22) and by Zangwill & Soven (23), who had performed the first time-dependent Kohn-Sham calculations.

It is the development of TDDFT in these past 20 years that we review in this article.



# THEORY

## Preliminaries

In this review we are concerned with systems described by the (nonrelativistic) many-body Schrödinger equation

$$\mathrm{i}\frac{\partial}{\partial t}\Psi(\{\boldsymbol{r}\}, t) = \hat{H}(\{\boldsymbol{r}\}, t)\Psi(\{\boldsymbol{r}\}, t), \quad (2)$$

where $\hat{H}$ is the Hamilton operator of the system and $\{\boldsymbol{r}\} = \{\boldsymbol{r}_1, \cdots, \boldsymbol{r}_N\}$ are the spatial coordinates of the $N$ electrons. This equation describes an initial value problem, i.e., if we know the state of the system at an initial time $t_0$, Equation 2 allows us to calculate $\Psi$ at any other time $t$. This is quite different from the solution of the time-independent Schrödinger equation, where our aim is to find the eigenstates of the Hamiltonian subject to some appropriate boundary conditions.

The Hamiltonian is naturally decomposed into three parts, $\hat{H}(\{\boldsymbol{r}\}, t) = \hat{T}(\{\boldsymbol{r}\}) + \hat{W}(\{\boldsymbol{r}\}) + \hat{V}_{\text{ext}}(\{\boldsymbol{r}\}, t)$. The first two are the kinetic energy and the electron-electron interaction,

$$\hat{T}(\{\boldsymbol{r}\}) = -\frac{1}{2}\sum_{i=1}^{N}\nabla_i^2, \qquad \hat{W}(\{\boldsymbol{r}\}) = \frac{1}{2}\sum_{\substack{i,j=1 \\ i\neq j}}^{N}\frac{1}{|\boldsymbol{r}_i - \boldsymbol{r}_j|}. \tag{3}$$

The third term can be written as a sum of one-body potentials,

$$\hat{V}_{\text{ext}}(\{\boldsymbol{r}\}, t) = \sum_{i=1}^{N} v_{\text{ext}}(\boldsymbol{r}_i, t), \tag{4}$$

and can be used, for example, to describe the Coulomb interaction of the electrons with a set of nuclei,

$$v_{\text{ext}}(\boldsymbol{r}, t) = -\sum_{\nu=1}^{N_{\text{n}}}\frac{Z_\nu}{|\boldsymbol{r} - \boldsymbol{R}_\nu(t)|}, \tag{5}$$

where $Z_\nu$ and $\boldsymbol{R}_\nu$ denote the charge and position of the nucleus $\nu$, and $N_{\text{n}}$ stands for the total number of nuclei in the system. Note that by allowing the $\boldsymbol{R}_\nu$ to depend on time we can treat situations where the nuclei move along a classical path. This may be useful to study, e.g., scattering experiments and chemical reactions. Another very interesting class of problems is the interaction of electrons with external time-dependent fields. For example, for a system illuminated by a laser beam we can write, in the dipole approximation,

$$v_{\text{ext}}(\boldsymbol{r}, t) = E f(t)\sin(\omega t)\boldsymbol{r}\cdot\boldsymbol{\alpha}, \tag{6}$$

where $\boldsymbol{\alpha}$, $\omega$, and $E$ are the polarization, the frequency, and the amplitude of the laser, respectively. The function $f(t)$ is an envelope that describes the temporal shape of the laser pulse.

The absolute square of the wave function $\Psi(\{\boldsymbol{r}\}, t)$ is interpreted as the probability of finding at time $t$ one electron at $\boldsymbol{r}_1$, another at $\boldsymbol{r}_2$, etc. It then follows that

$$n(\boldsymbol{r}, t) = N\int \mathrm{d}^3\boldsymbol{r}_2\cdots\mathrm{d}^3\boldsymbol{r}_N\,|\Psi(\boldsymbol{r}, \boldsymbol{r}_2\cdots\boldsymbol{r}_N, t)|^2 \tag{7}$$

gives $N$ times the probability of finding an electron at time $t$ and position $\boldsymbol{r}$. With this definition, the density $n(\boldsymbol{r}, t)$ is normalized at all times to the total number of

electrons, $N$. This quantity, the electronic density $n(\boldsymbol{r}, t)$, is the basic variable in terms of which TDDFT is formulated.

## Basic Theorems

The central theorem of TDDFT (now called the Runge-Gross theorem) proves that there is a one-to-one correspondence between the external (time-dependent) potential, $v_{\text{ext}}(\boldsymbol{r}, t)$, and the electronic density, $n(\boldsymbol{r}, t)$, for many-body systems evolving from a fixed initial state (21). This is a nontrivial statement with profound consequences. It implies that, if the only information we have about the system is its density, we can obtain the external potential that produced this density. With the external potential the time-dependent Schrödinger equation can be solved, and all properties of the system obtained. From this we conclude that the electronic density determines all other properties of the quantum system. Note that this statement is true for a fixed initial state, i.e, besides the knowledge of $n(\boldsymbol{r}, t)$ we also need to know the initial many-body state. The situation is somewhat different if the system departs from its ground state: By virtue of the ordinary Hohenberg-Kohn theorem, the many-body ground state is uniquely determined by the initial density, $n(\boldsymbol{r}, t = t_0)$. If, however, the system at $t = t_0$ is in a arbitrary state, the knowledge of the initial state is essential (24, 25).

The proof of the Runge-Gross theorem is considerably more involved than the proof of the ordinary Hohenberg-Kohn theorem. The statement actually proved is that no two potentials, $v(\boldsymbol{r}, t)$ and $v'(\boldsymbol{r}, t)$, differing by more than a purely time-dependent function $c(t)$[1], can produce the same time-dependent density, $n_\sigma(\boldsymbol{r}, t)$. The demonstration is divided into parts: First, one proves, using the equation of motion for the current density, that if $v \neq v' + c(t)$, then the current densities, $\boldsymbol{j}$ and $\boldsymbol{j}'$, generated by $v$ and $v'$, are also different. In a second step, it is demonstrated that if two systems have different current densities, then they must also possess different time-dependent densities, i.e, $\boldsymbol{j} \neq \boldsymbol{j}' \Rightarrow n \neq n'$. This proof is accomplished with the help of the continuity equation. The original proof requires that the external potential can be expanded for $t > t_0$ in a Taylor series around the initial time $t_0$. This is a fairly mild requirement (certainly fulfilled by all physical potentials). It excludes, however, the mathematically important case of adiabatically switched-on potentials. Further (mild) conditions on the allowable $\boldsymbol{r}$ dependence were discussed in detail by Gross & Kohn (15).

In possession of the Runge-Gross theorem, it is fairly straightforward to construct a time-dependent Kohn-Sham scheme. We introduce an auxiliary system of noninteracting electrons subject to an external local potential $v_{\text{KS}}$. This potential is unique, by virtue of the Runge-Gross theorem applied to the noninteracting system, and is chosen such that the density of the Kohn-Sham electrons is the same as the density of the original interacting system. These Kohn-Sham electrons obey

[1]If the two potentials differ solely by a time-dependent function, they produce wave functions that are equal up to a purely time-dependent phase. This phase, of course, is canceled when the density (or any other observable, in fact) is calculated.

the time-dependent Schrödinger equation

$$\mathrm{i}\frac{\partial}{\partial t}\varphi_i(\boldsymbol{r},t) = \hat{H}_{\mathrm{KS}}(\boldsymbol{r},t)\varphi_i(\boldsymbol{r},t), \tag{8}$$

where the Kohn-Sham Hamiltonian is defined as

$$\hat{H}_{\mathrm{KS}}(\boldsymbol{r},t) = -\frac{\nabla^2}{2} + v_{\mathrm{KS}}[n](\boldsymbol{r},t). \tag{9}$$

By construction, the density of the interacting system can then be calculated from the Kohn-Sham orbitals

$$n(\boldsymbol{r},t) = \sum_i^N |\varphi_i(\boldsymbol{r},t)|^2 . \tag{10}$$

As in the Kohn-Sham scheme for the ground state, the time-dependent Kohn-Sham potential is normally written as the sum of three terms

$$v_{\mathrm{KS}}[n](\boldsymbol{r},t) = v_{\mathrm{ext}}(\boldsymbol{r},t) + v_{\mathrm{Hartree}}[n](\boldsymbol{r},t) + v_{\mathrm{xc}}[n](\boldsymbol{r},t). \tag{11}$$

The first term is the external potential, whereas the second accounts for the classical electrostatic interaction between the electrons

$$v_{\mathrm{Hartree}}(\boldsymbol{r},t) = \int \mathrm{d}^3r' \frac{n(\boldsymbol{r},t)}{|\boldsymbol{r}-\boldsymbol{r}'|}. \tag{12}$$

The third term, the xc potential, includes all nontrivial many-body effects, and has an extremely complex (and essentially unknown) functional dependence on the density. This dependence is clearly nonlocal, both in space and in time, i.e., the potential at time $t$ and position $\boldsymbol{r}$ can depend on the density at all other positions and all previous times (due to causality). Note that the way of writing (11) is largely a matter of convention. We separate out of $v_{\mathrm{KS}}$ two large terms that are well known, the external and Hartree potentials, and write the rest as the "mysterious" xc term that we expect to approximate using clever physical and mathematical arguments. The quality of the results obviously depends on the quality of the approximation to the xc potential used. It is important to stress that, like in ground-state density functional theory, this is the only fundamental approximation in TDDFT.

Formally, not only is $v_{\mathrm{xc}}$ a functional of the density, but it also depends on the initial Kohn-Sham determinant and on the initial many-body wave function. For practical reasons the latter dependence is always neglected. Explicit density functionals, like the adiabatic LDA, only retain the density dependence. Orbital functionals, on the other hand, are functionals of both the time-dependent density and the initial Kohn-Sham determinant.

At the heart of the Kohn-Sham construction lies the assumption that there exists a noninteracting system that possesses the same density as the interacting system that we are interested in. If this is the case, the interacting density is said to be non-interacting $v$-representable. For ground-state DFT it is well known that there are

some smooth densities that are not noninteracting *v*-representable by a single determinant [the known examples are densities built from degenerate ensembles (26, 27)]. Curiously, the situation is much more satisfactory in TDDFT: it was shown that, under very mild assumptions, a time-dependent one-body potential $v_{\rm KS}(\boldsymbol{r}, t)$ exists that reproduces a given smooth density $n(\boldsymbol{r}, t)$ at all times (28). Of course, we still need to assume that the initial state is noninteracting *v*-representable.

## Causality and the Quantum-Mechanical Action



In quantum mechanics, the ground state of a system can be determined through the minimization of the total energy. In time-dependent systems there can be no variational principle based on the total energy, simply because the total energy is not a conserved quantity. There exists, however, a quantity analogous to the energy, the quantum mechanical action

$$\mathcal{A}[\Psi] = \int_{t_0}^{t_1} \mathrm{d}t \ \langle \Psi(t)| \, \mathrm{i}\frac{\partial}{\partial t} - \hat{H}(t) \, |\Psi(t)\rangle \,, \tag{13}$$

where $\Psi(t)$ is an *N*-body function defined in some convenient space. It is clearly seen that $\delta\mathcal{A}/\delta \langle \Psi(t)|$ yields the time-dependent Schrödinger equation. In their original paper, Runge & Gross (21) offered a derivation of the Kohn-Sham equations starting from the action (13). The xc potential is then simply the functional derivative

$$v_{\rm xc}(\boldsymbol{r}, t) = \frac{\delta \mathcal{A}_{\rm xc}}{\delta n(\boldsymbol{r}, t)}, \tag{14}$$

where $\mathcal{A}_{\rm xc}$ includes all nontrivial many-body parts of the action. However, it was later discovered that this formulation encompasses two fundamental problems: (*a*) Response functions like $f_{\rm xc}(\boldsymbol{r}t, \boldsymbol{r}'t') = \delta v_{\rm xc}(\boldsymbol{r}, t)/\delta n(\boldsymbol{r}', t')$ must be causal, i.e., must be zero for $t < t'$, but Equation 13 leads to an $f_{\rm xc}$ which is a symmetric function of its time (and space) arguments, and therefore not causal (29, 16). (*b*) To derive the time-dependent Schrödinger equation from (Equation 13) we must impose two boundary conditions on the variation, $\delta\Psi(t_0) = \delta\Psi(t_1) = 0$. However, these two variations are not independent within TDDFT, as the value of $\delta\Psi(t_1)$ is fully determined by $\delta\Psi(t_0) = 0$ (30, 17). These two problems were solved by van Leeuwen (30) in 1998. The causality problem is circumvented by the use of the Keldysh formalism (31), while the second problem is resolved by introducing a new action functional that does not explicitly contain $\partial/\partial t$:

$$A[n] = -\mathrm{i} \ln \langle \Psi(t_0)| \, \hat{U}(\tau_f, \tau_i) \, |\Psi(t_0)\rangle + \int_{\tau_0}^{\tau_1} \mathrm{d}\tau t'(\tau) \int \mathrm{d}^3 r n(\boldsymbol{r}, \tau) v_{\rm ext}(\boldsymbol{r}, \tau), \tag{15}$$

where $\tau$ stands for the Keldysh pseudotime, $t'(\tau)$ is a shorthand for $\mathrm{d}t/\mathrm{d}\tau$, and $U$ is the evolution operator of the system

$$\hat{U}(\tau_f, \tau_i) = \hat{T}_C \exp\left[-\mathrm{i}\int_{\tau_0}^{\tau_1} \mathrm{d}\tau t'(\tau)\hat{H}(\tau)\right]. \tag{16}$$

In the last expression, $\hat{T}_C$ denotes ordering in $\tau$. Using the action functional (15), it is possible to construct a system of noninteracting (Kohn-Sham) electrons that yields the same time-dependent density as the interacting system. The action of the Kohn-Sham system, $A_{\mathrm{KS}}$, is defined similarly as in (15) but with $\hat{H}$ replaced by $\hat{H}_{\mathrm{KS}}$. The xc part of the action functional can then be defined through the relation

$$A[n] = A_{\mathrm{KS}}[n] - A_{\mathrm{xc}}[n] - \frac{1}{2}\int_{\tau_0}^{\tau_1} \mathrm{d}\tau t'(\tau) \int \mathrm{d}^3\mathrm{r} \int \mathrm{d}^3\mathrm{r}' \frac{n(\boldsymbol{r}, \tau)n(\boldsymbol{r}', \tau)}{|\boldsymbol{r} - \boldsymbol{r}'|}. \tag{17}$$

The xc potential is given by the functional derivative (note the difference to Equation 14)

$$v_{\mathrm{xc}}(\boldsymbol{r}, t) = \left.\frac{\delta A_{\mathrm{xc}}[n]}{\delta n(\boldsymbol{r}, \tau)}\right|_{n=n(\boldsymbol{r},t)}. \tag{18}$$

We can now see how the causality problem is resolved: Response functions will be symmetric in the Keldysh pseudotime, $\tau$, but properly causal when converted to real time.

## Exchange-Correlation Potentials

In this section we review the approximate xc functionals available in TDDFT. To this end we switch to the spin-dependent version of TDDFT, which was derived by Liu & Vosko (32) in 1989. In this generalization, the xc potentials, $v_{\mathrm{xc}\sigma}[n_\uparrow, n_\downarrow](\boldsymbol{r}, t)$, for spin up ($\sigma = \uparrow$) and spin down ($\sigma = \downarrow$) electrons depend on the time-dependent spin densities $n_\uparrow(\boldsymbol{r}, t)$ and $n_\downarrow(\boldsymbol{r}, t)$.

The history of xc functionals in ground-state DFT starts with the local (spin) density approximation (LDA) (5). In the LDA the xc energy density at each point in space is approximated by the xc energy density of a homogeneous electron gas (6) with spin densities $n_\sigma(\boldsymbol{r})$.

$$E_{\mathrm{xc}}^{\mathrm{LDA}}[n_\uparrow, n_\downarrow] = \int \mathrm{d}^3 r n(\boldsymbol{r}) e_{\mathrm{xc}}^{\mathrm{HEG}}(n_\uparrow, n_\downarrow). \tag{19}$$

The LDA potential is local, i.e., the value of the potential at position $\boldsymbol{r}$ depends solely on the value of the spin densities at the very same point. This simple approximation has turned out to be quite reliable. In the next generation of functionals, the generalized gradient approximations (GGA) (33), the xc energy density is written as a function of the density and of its gradient, $\nabla n_\sigma$,

$$E_{\mathrm{xc}}^{\mathrm{GGA}}[n_\uparrow, n_\downarrow] = \int \mathrm{d}^3 r n(\boldsymbol{r}) e_{\mathrm{xc}}^{\mathrm{GGA}}(n_\uparrow, n_\downarrow, \nabla n_\uparrow, \nabla n_\downarrow). \tag{20}$$

The GGAs are presently the functionals of choice in quantum chemistry, but the LDA is still more widely used in solid-state physics. Recently, a more general class of functionals was proposed—the meta-GGAs (34)

$$E_{\rm xc}^{\rm MGGA}[n_\uparrow, n_\downarrow] = \int {\rm d}^3 r\, n(\boldsymbol{r}) e_{\rm xc}^{\rm GGA}(n_\uparrow, n_\downarrow, \nabla n_\uparrow, \nabla n_\downarrow, \nabla^2 n_\uparrow, \nabla^2 n_\downarrow, \tau_\uparrow, \tau_\downarrow), \quad (21)$$

where $\tau_\sigma(\boldsymbol{r}) = \sum_i |\nabla \varphi_{i\sigma}(\boldsymbol{r})|^2$ denotes the kinetic energy density. The added ingredients had been previously recognized by Becke (35–37) as natural quantities from several points of view. Owing to the explicit dependence on $\tau_\sigma$, the meta-GGAs are orbital functionals, i.e., they have an explicit dependence on the Kohn-Sham orbitals. Of course, we should not forget that the Kohn-Sham orbitals are themselves functionals of the density (by virtue of the Hohenberg-Kohn theorem), so the meta-GGAs are still implicit density functionals. Other orbital functionals exist on the market, such as the exact exchange (EXX) (38, 39), the self-interaction corrected LDA (SIC-LDA) (40), or the interaction strength interpolation (ISI) (41).

This plethora of functionals is the result of more than 35 years of active research. Unfortunately, and in contrast to stationary-state DFT, approximations to the time-dependent xc potential are still in their infancy. The simplest approximation is the so-called adiabatic approximation

$$v_{{\rm xc}\sigma}^{\rm adiabatic}[n_\uparrow, n_\downarrow](\boldsymbol{r}, t) = \tilde{v}_{{\rm xc}\sigma}[n_\uparrow, n_\downarrow](\boldsymbol{r})|_{n_\sigma = n_\sigma(\boldsymbol{r}, t)}, \quad (22)$$

where $\tilde{v}_{{\rm xc}\sigma}[n_\uparrow, n_\downarrow]$ is some given ground-state xc functional. This adiabatic functional is clearly local in time. As $\tilde{v}_{{\rm xc}\sigma}[n_\uparrow, n_\downarrow]$ is a ground-state property, we expect that the adiabatic approximation works best for time-dependent systems that only slightly deviate from their ground state. By inserting the LDA potential in Equation 22, we obtain the adiabatic local density approximation (ALDA), which is perhaps the most widely used functional in TDDFT. Naturally, the ALDA retains all the problems already present in the LDA. One of those problems, particularly important in time-dependent systems where the electrons are pushed to regions far away from the nuclei, is the incorrect asymptotic behavior of the LDA potential. For neutral finite systems, the exact xc potential decays as $-1/r$ while the LDA potential goes to zero exponentially. Unfortunately, this problem is not corrected by most of the GGAs [an exception is the van Leeuwen & Baerends functional (LB94) (42)], nor by the more modern meta-GGAs.

A functional that does exhibit the correct asymptotic behavior is the EXX. The EXX action is obtained by expanding $A_{\rm xc}$ to first order in $e^2$ (where $e$ denotes the electron charge). It is given by the Fock integral (43, 30)

$$A_{\rm x}^{\rm EXX} = -\frac{1}{2} \sum_\sigma \sum_{j,k}^{\rm occ} \int_{\tau_0}^{\tau_1} {\rm d}\tau t'(\tau) \int {\rm d}^3 {\rm r} \int {\rm d}^3 {\rm r}' \frac{\varphi_{j\sigma}^*(\boldsymbol{r}', \tau)\varphi_{k\sigma}(\boldsymbol{r}', \tau)\varphi_{j\sigma}(\boldsymbol{r}, \tau)\varphi_{k\sigma}^*(\boldsymbol{r}, \tau)}{|\boldsymbol{r} - \boldsymbol{r}'|}. \quad (23)$$

As this action is not an explicit density functional, one has to go through a series of chain rules in order to obtain $v_{\mathrm{x}}^{\mathrm{EXX}}$. The procedure is known, for historical reasons, as the optimized effective potential (OEP) or the optimized potential method (OPM) (38, 39). This method was generalized to the time-dependent case by Ullrich et al. (43). The EXX potential is then determined by solving the integral equation

$$\sum_{j}^{\mathrm{occ}} \int \mathrm{d}t' \int \mathrm{d}^3 r' \left[ v_{\mathrm{x}\sigma}^{\mathrm{EXX}}(\boldsymbol{r}', t') - u_{\mathrm{x}j\sigma}(\boldsymbol{r}', t') \right] \times \varphi_{j\sigma}(\boldsymbol{r}, t) \varphi_{j\sigma}^{*}(\boldsymbol{r}', t') G_{\mathrm{R}\sigma}(\boldsymbol{r}t, \boldsymbol{r}'t') + \mathrm{c.c.} = 0, \tag{24}$$

where we have defined the retarded Green's function by

$$\mathrm{i} G_{\mathrm{R}\sigma}(\boldsymbol{r}t, \boldsymbol{r}'t') = \theta(t - t') \sum_{k=1}^{\infty} \varphi_{k\sigma}^{*}(\boldsymbol{r}, t) \varphi_{k\sigma}(\boldsymbol{r}', t'). \tag{25}$$

The function $u_{\mathrm{x}j\sigma}$ is essentially the functional derivative of the action functional in terms of the Kohn-Sham orbital $j$

$$u_{\mathrm{x}j\sigma}(\boldsymbol{r}, t) = \frac{1}{\varphi_{j\sigma}^{*}(\boldsymbol{r}, t)} \left. \frac{\delta A_{\mathrm{x}}^{\mathrm{EXX}}[\varphi_{j\sigma}]}{\delta \varphi_{j\sigma}(\boldsymbol{r}, \tau)} \right|_{\varphi_{j\sigma} = \varphi_{j\sigma}(\boldsymbol{r}, t)}. \tag{26}$$

Note that the xc potential is still a local potential, even though it is obtained through the solution of an extremely nonlocal and nonlinear integral equation. It is possible to obtain a semianalytic solution of Equation 24 by generalizing to the time-dependent case (43) an approximation first proposed by Krieger, Lee & Iafrate (KLI) (44). The KLI potential retains the correct asymptotic behavior of $v_{\mathrm{x}}^{\mathrm{EXX}}$, but its dependence on the Kohn-Sham orbitals becomes local in the time coordinate.

There have been few attempts to derive a functional which is nonlocal in time, i.e., that includes the "memory" of previous times. In 1997, Dobson et al. (45) constructed one such functional by borrowing a concept from hydrodynamics. They assumed that in the electron liquid memory resides not with each fixed point $\boldsymbol{r}$, but rather within each separate "fluid element". Thus the element that arrives at location $\boldsymbol{r}$ at time $t$ "remembers" what happened to it at earlier times when it was at locations different from its present location $\boldsymbol{r}$. Using this concept, Dobson et al. proposed a functional that satisfies Galilean invariance and Ehrenfest's theorem. Unfortunately, no applications of this functional exist to date.

## LINEAR RESPONSE THEORY

### Generalities

One of the corollaries of the Hohenberg-Kohn theorem for the ground state is that all observables are functionals of the density (1). In fact, from the knowledge of the density it is possible to uniquely determine the external potential. With this

potential we can, in principle, solve the many-body Schrödinger equation, and from the many-body energies and eigenfunctions determine all observables. Clearly, also the energies of the excited states can be viewed in this way, i.e., they are functionals of the ground-state density. Unfortunately, the Hohenberg-Kohn theorem is only an existence proof, and does not teach us how to write the functionals explicitly. In general, and with few exceptions, we have little or no information on how to express an observable as a functional of the ground-state density. This is also the case for the excitation energies of the system. To circumvent this problem, several approaches within the scope of DFT have been proposed over the years. Some are more or less ad hoc, others rely on a solid theoretical basis. Moreover, the degree of success varies considerably among the different techniques.

As a first approximation to the excitation energies one usually uses the differences between the ground-state Kohn-Sham eigenvalues. It is well known that the Kohn-Sham eigenvalues do not have any strict physical meaning [with the exception of the highest occupied one (46)], but, in cases where no other calculations are available, they are often used to interpret experimental observations. More elaborate approaches include (*a*) restricting the variational principle to wave functions of a specified symmetry, thereby obtaining the energy of the lowest state for every symmetry class (47); (*b*) the so-called generalized adiabatic connection Kohn-Sham formalism, where each state of the many-body system is adiabatically connected to a Kohn-Sham state (48, 49); (*c*) searching for local extrema of the ground-state energy functional (50); and (*d*) calculating multiplet energies by a Hartree-Fock-Slater method (51).

Another very interesting technique is ensemble DFT (52–57). In this method we are concerned with "ensembles" of the ground state with some excited states. In the simplest case, the ensemble is defined by the density matrix

$$\hat{D} = (1-\omega)\,|\Psi_1\rangle\,\langle\Psi_1| + \omega\,|\Psi_2\rangle\,\langle\Psi_2|\,, \tag{27}$$

where $\Psi_1$ is the ground state and $\Psi_2$ the lowest excited state, and $\omega$ is some given weight between 0 and $1/2$. Using the ensemble density it is then possible to construct a DFT, and obtain the ensemble energy $E(\omega)$ from solving a set of Kohn-Sham-like equations. Knowing $E(\omega)$ and the ground-state energy (which can be obtained from ordinary DFT) it is trivial to determine the energy of the first excited state. The procedure can obviously be continued to calculate all excited-state energies. The culprit of ensemble DFT (as in any other DFT) is the existence of good xc functionals. An ensemble LDA was developed for the equiensemble (i.e., an ensemble with $\omega = 1/2$) by Kohn in 1986 (58), but the results obtained with this functional were not very encouraging. A more promising approach, involving orbital functionals within an ensemble OEP method, has also been proposed recently (59, 60).

Alternatively, the excitation energies can be obtained by knowing how the system responds to a small time-dependent perturbation, and can therefore be readily extracted from a TDDFT calculation.

## The Photoabsorption Spectrum

For a finite system the photoabsorption cross section is proportional to the imaginary part of the dynamic polarizability.

$$\sigma(\omega) = \frac{4\pi\omega}{c}\frac{1}{3}\Im\sum_{\gamma}\alpha_{\gamma}(\omega), \tag{28}$$

where $c$ denotes the speed of light, $\gamma = x, y, z$, and $\alpha_{\gamma}(\omega)$ is simply given by

$$\alpha_{\gamma}(\omega) = -\int \mathrm{d}^3r \int \mathrm{d}^3r' r_{\gamma} \sum_{\sigma\sigma} \chi_{\sigma\sigma}(\boldsymbol{r}, \boldsymbol{r}', \omega) r'_{\gamma}. \tag{29}$$

The function $\chi$, the so-called linear density response function of the system, measures the change of the density when the system is perturbed by a small (infinitesimal) change of the external potential

$$\delta n_{\sigma}(\boldsymbol{r}, \omega) = \sum_{\sigma'} \int \mathrm{d}^3r' \chi_{\sigma\sigma'}(\boldsymbol{r}, \boldsymbol{r}', \omega) \delta v_{\mathrm{ext}\sigma'}(\boldsymbol{r}', \omega). \tag{30}$$

A prescription on how to calculate the photoabsorption spectrum is as follows (61): Let $\{\tilde{\varphi}_{j\sigma}(\boldsymbol{r})\}$ be the ground-state Kohn-Sham wave functions of the system. Apply a perturbation of the form $\delta v_{\mathrm{ext}\sigma}(\boldsymbol{r}, t) = -\kappa_0 r_{\nu}\delta(t)$. The amplitude $\kappa_0$ must be small in order to keep the response of the system linear. This perturbation excites all frequencies of the system with equal weight. At $t = 0^+$ the Kohn-Sham orbitals are

$$\varphi_{j\sigma}(\boldsymbol{r}, t = 0^+) = \mathrm{e}^{\mathrm{i}\kappa_0 r_{\gamma}} \tilde{\varphi}_{j\sigma}(\boldsymbol{r}). \tag{31}$$

These orbitals are then further propagated for a finite time. The dynamical polarizability can then be obtained from

$$\alpha_{\gamma}(\omega) = -\frac{1}{\kappa_0}\int \mathrm{d}^3r r_{\gamma}\delta n(\boldsymbol{r}, \omega). \tag{32}$$

In the previous expression, $\delta n(\boldsymbol{r}, \omega)$ stands for the time Fourier transform of $n(\boldsymbol{r}, t) - \tilde{n}(\boldsymbol{r})$, where $\tilde{n}(\boldsymbol{r})$ is the ground-state density of the system. This prescription has been used with considerable success to calculate the photoabsorption spectrum of several finite systems, from small molecules [see, e.g., References 62 and 63] to biological systems (64). As it is based on the propagation of the Kohn-Sham equations, this approach can be easily extended to study nonlinear responses, or to treat cases where the external field is not a small perturbation. However, if our sole objective is the calculation of the linear excitation spectrum, it is possible to use linear response theory to evaluate $\chi$ directly.

## Kohn-Sham Linear Response Theory

Equation 30 tells us how to calculate the change in density, $\delta n$, from a change in the external potential $\delta v_{\mathrm{ext}}$. Clearly, we can calculate the same change in density

using the Kohn-Sham system

$$\delta n_\sigma(\boldsymbol{r},\omega)=\sum_{\sigma'}\int \mathrm{d}^3r'\,\chi_{\mathrm{KS}\sigma\sigma'}(\boldsymbol{r},\boldsymbol{r}',\omega)\delta v_{\mathrm{KS}\sigma'}(\boldsymbol{r}',\omega). \tag{33}$$

The response function that enters Equation 33 is the density response function of the noninteracting Kohn-Sham electrons. In terms of the unperturbed stationary Kohn-Sham orbitals it reads

$$\chi_{\mathrm{KS}\sigma\sigma'}(\boldsymbol{r},\boldsymbol{r}',\omega)=\delta_{\sigma\sigma'}\sum_{jk}^{\infty}(f_{k\sigma}-f_{j\sigma})\frac{\varphi_{j\sigma}(\boldsymbol{r})\varphi^*_{j\sigma}(\boldsymbol{r}')\varphi_{k\sigma}(\boldsymbol{r}')\varphi^*_{k\sigma}(\boldsymbol{r})}{\omega-(\epsilon_{j\sigma}-\epsilon_{k\sigma})+\mathrm{i}\eta}, \tag{34}$$

where $\varphi_{j\sigma}$ and $\epsilon_{j\sigma}$ are the ground-state Kohn-Sham orbitals and eigenvalues, $f_j$ is the occupation number of the $j$th orbital, and $\eta$ is a positive infinitesimal. Using the definition of the Kohn-Sham potential, Equation 11, we can obtain the linear change of the Kohn-Sham potential

$$\begin{aligned}\delta v_{\mathrm{KS}\sigma}(\boldsymbol{r},\omega)=\delta v_{\mathrm{ext}\sigma}(\boldsymbol{r},\omega)+\int \mathrm{d}^3r'\frac{\delta n(\boldsymbol{r}',\omega)}{|\boldsymbol{r}-\boldsymbol{r}'|}\\ +\sum_{\sigma'}\int \mathrm{d}^3r'\,f_{\mathrm{xc}\sigma\sigma'}(\boldsymbol{r},\boldsymbol{r}',\omega)\delta n_{\sigma'}(\boldsymbol{r}',\omega),\end{aligned} \tag{35}$$

with $\delta n=\delta n_\uparrow+\delta n_\downarrow$, and where we have introduced the time Fourier transform of the xc kernel

$$f_{\mathrm{xc}\sigma\sigma'}[n_\uparrow,n_\downarrow](\boldsymbol{r},\boldsymbol{r}',t-t')=\frac{\delta v_{\mathrm{xc}\sigma}[n_\uparrow,n_\downarrow](\boldsymbol{r},t)}{\delta n_{\sigma'}(\boldsymbol{r}',t')}. \tag{36}$$

Combining the previous results we obtain

$$\begin{aligned}\delta n_\sigma(\boldsymbol{r},\omega)=\sum_\tau\int \mathrm{d}^3r'\chi_{\mathrm{KS}\sigma\tau}(\boldsymbol{r},\boldsymbol{r}',\omega)\Bigg[\delta v_{\mathrm{ext}\tau}(\boldsymbol{r}',\omega)+\int \mathrm{d}^3x\frac{\delta n(\boldsymbol{x},\omega)}{|\boldsymbol{r}'-\boldsymbol{x}|}\\ +\sum_{\tau'}\int \mathrm{d}^3x\,f_{\mathrm{xc}\tau\tau'}(\boldsymbol{r}',\boldsymbol{x},\omega)\delta n_{\tau'}(\boldsymbol{x},\omega)\Bigg].\end{aligned} \tag{37}$$

Inserting Equation 30 and using the fact that $\delta v_{\mathrm{ext}}$ is an arbitrary function, we arrive at a Dyson-like equation for the response function

$$\begin{aligned}\chi_{\sigma\sigma'}(\boldsymbol{r},\boldsymbol{r}',\omega)=\chi_{\mathrm{KS}\sigma\sigma'}(\boldsymbol{r},\boldsymbol{r}',\omega)\\ +\sum_{\tau\tau'}\int \mathrm{d}^3x\int \mathrm{d}^3x'\chi_{\sigma\tau}(\boldsymbol{r},\boldsymbol{x},\omega)\left[\frac{1}{|\boldsymbol{x}-\boldsymbol{x}'|}+f_{\mathrm{xc}\tau\tau'}(\boldsymbol{x},\boldsymbol{x}',\omega)\right]\chi_{\mathrm{KS}\tau'\sigma'}(\boldsymbol{x}',\boldsymbol{r}',\omega).\end{aligned} \tag{38}$$

Equation 38 gives a formally exact representation of the density response of the interacting system. In fact, if we were in possession of the exact functional $f_{\mathrm{xc}}[n_\uparrow,n_\downarrow]$, a self-consistent solution of Equation 38 would yield the response

function, $\chi$, of the interacting system. We note that by putting $f_{\mathrm{xc}} = 0$ one recovers the random phase approximation (RPA) to the response function.

As we have established, the key ingredient of Equation 38 is the xc kernel, $f_{\mathrm{xc}}$. This is, as expected, a very complicated functional of the density that encompasses all nontrivial many-body effects of the system. The simplest approximation to $f_{\mathrm{xc}}$ is the ALDA kernel

$$f_{\mathrm{xc}\sigma\sigma'}^{\mathrm{ALDA}}(\boldsymbol{r}t, \boldsymbol{r}'t') = \delta(\boldsymbol{r} - \boldsymbol{r}')\delta(t - t')\, f_{\mathrm{xc}\sigma\sigma'}^{\mathrm{HEG}}(n_\uparrow, n_\downarrow)|_{n_\sigma = n_\sigma(\boldsymbol{r},t)}, \tag{39}$$

where

$$f_{\mathrm{xc}\sigma\sigma'}^{\mathrm{HEG}}(n_\uparrow, n_\downarrow) = \frac{\mathrm{d}}{\mathrm{d}n_{\sigma'}} v_{\mathrm{xc}\sigma}^{\mathrm{HEG}}(n_\uparrow, n_\downarrow) \tag{40}$$

is just the derivative of the xc potential of the homogeneous electron gas. This kernel is trivially derived by using the ALDA xc potential in the definition (36). Note that the ALDA kernel is local both in space and in time (and hence, obviously causal).

Despite being a very crude approximation, it is found that the ALDA yields very good results for a large variety of molecules and clusters. This apparent paradox was studied in 1985 by Gross & Kohn, who compared the ALDA kernel with an approximation to the long wavelength limit (but still frequency dependent) $f_{\mathrm{xc}}$ for the electron gas, $f_{\mathrm{xc}}^{\mathrm{HEG}}(\boldsymbol{q} \to 0, \omega)$ (65). This approximation was built with the help of several known limits and symmetry properties of $f_{\mathrm{xc}}^{\mathrm{HEG}}$. By construction, the ALDA is a good approximation at low frequencies, but at higher frequencies it completely fails to reproduce the behavior of $f_{\mathrm{xc}}^{\mathrm{HEG}}$ (especially at lower densities). The ALDA yields such good excitation energies, even at high frequencies, because excitations at these high frequencies are usually connected to regions of space with a large density of electrons, where the ALDA becomes again a good approximation.

Another commonly used xc kernel was derived by Petersilka et al. in 1996 (66, 67) starting from a simple analytical approximation to the EXX potential. This approximation, called the Slater approximation in the context of Hartree-Fock theory, retains only the leading term in the expression for EXX. The final form of the PGG kernel is

$$f_{\mathrm{x}\sigma\sigma'}^{\mathrm{PGG}}(\boldsymbol{r}t, \boldsymbol{r}'t') = -\delta(t - t')\delta_{\sigma\sigma'} \frac{1}{|\boldsymbol{r} - \boldsymbol{r}'|} \frac{\left|\sum_k f_{k\sigma}\varphi_{k\sigma}(\boldsymbol{r})\varphi_{k\sigma}^*(\boldsymbol{r}')\right|^2}{n_\sigma(\boldsymbol{r})n_\sigma(\boldsymbol{r}')}. \tag{41}$$

This kernel is again local in time, but has a nonlocal spatial dependence.

Several other xc kernels have been proposed in the past few years (68–72). The interested reader may find a list with a short description of each kernel in Reference 18.

## The Poles of the Response Function

Unfortunately, a full solution of Equation 38 is still quite difficult numerically. Furthermore, it requires the knowledge of the noninteracting response function (34).

The evaluation of this function is normally performed through an infinite summation over both the occupied and the unoccupied parts of the spectrum. This summation is sometimes slowly convergent and requires the inclusion of many unoccupied states. For systems with a discrete spectrum of excitation (like finite systems) it is possible to recast Equation 38 into a form that avoids these inconveniences (66). The starting point is the Lehmann representation of the density response function

$$\chi_{\sigma\sigma'}(\boldsymbol{r},\boldsymbol{r}',\omega) = \lim_{\eta\to 0^+}\sum_m\left[\frac{\langle 0|\,\hat{n}_\sigma(\boldsymbol{r})\,|m\rangle\,\langle m|\,\hat{n}_{\sigma'}(\boldsymbol{r}')\,|0\rangle}{\omega-(E_m-E_0)+\mathrm{i}\eta}-\frac{\langle 0|\,\hat{n}_{\sigma'}(\boldsymbol{r}')\,|m\rangle\,\langle m|\,\hat{n}_\sigma(\boldsymbol{r})\,|0\rangle}{\omega+(E_m-E_0)+\mathrm{i}\eta}\right], \tag{42}$$

where $\hat{n}$ is the density operator, $|m\rangle$ forms a complete set of many-body states with energies $E_m$, and $\eta$ is a positive infinitesimal. From this expression it is evident that the full density response function has poles at frequencies that correspond to the excitation energies of the interacting system

$$\Omega = E_m - E_0. \tag{43}$$

In the same way it is simple to realize that the Kohn-Sham response function, $\chi_{\mathrm{KS}}$, has poles at the difference of Kohn-Sham eigenvalues, $\epsilon_{j\sigma}-\epsilon_{k\sigma}$ (see Equation 34). With this information it is possible, starting from Equation 38 and through a series of algebraic manipulations (73), to arrive at a pseudo eigenvalue equation that determines the excitation energies (43)

$$\sum_{j'k'\sigma'}[\delta_{jj'}\delta_{kk'}\delta_{\sigma\sigma'}\omega_{jk\sigma}+(f_{k'\sigma'}-f_{j'\sigma'})K_{jk\sigma,j'k'\sigma'}(\Omega)]\beta_{j'k'\sigma'}=\Omega\beta_{jk\sigma}, \tag{44}$$

where we have defined $\omega_{jk\sigma}=\epsilon_{j\sigma}-\epsilon_{k\sigma}$ and

$$K_{jk\sigma,j'k'\sigma'}(\omega) = \int \mathrm{d}^3r\int \mathrm{d}^3r'\varphi^*_{j\sigma}(\boldsymbol{r})\varphi_{k\sigma}(\boldsymbol{r})\left[\frac{1}{|\boldsymbol{r}-\boldsymbol{r}'|}+f_{\mathrm{xc}\sigma\sigma'}(\boldsymbol{r},\boldsymbol{r}',\omega)\right]\varphi_{j'\sigma'}(\boldsymbol{r}')\varphi^*_{k'\sigma'}(\boldsymbol{r}'). \tag{45}$$

Note that Equation 44 gives the exact position of the poles of the density response function, i.e., the excitation energies of the system, and does not involve any further approximation. If the excitation is well-described by one single-particle transition between an occupied and a virtual state, we can neglect the off-diagonal terms of $K_{jk\sigma,j'k'\sigma'}$ to obtain the single-pole approximation (SPA) to the excitation energies (66). For a spin-unpolarized system it reads

$$\Omega=\omega_{12}+\Re[K_{12\uparrow,12\uparrow}\pm K_{12\uparrow,12\downarrow}]. \tag{46}$$

Two details should be noticed in the previous formula: (*a*) The Coulomb and $f_{\mathrm{xc}}$ contributions to the excitation energy appear as an additive correction to the

Kohn-Sham eigenvalue differences; (*b*) Equation 46 describes properly the spin-multiplet structure of otherwise spin-unpolarized ground states through the spin-dependence of $f_{\mathrm{xc}}$. To make this fact more evident, we can perform the transformation $f_{\mathrm{xc}}^{(1)} = (f_{\mathrm{xc}\uparrow\uparrow} + f_{\mathrm{xc}\uparrow\downarrow})/2$ and $f_{\mathrm{xc}}^{(2)} = (f_{\mathrm{xc}\uparrow\uparrow} - f_{\mathrm{xc}\uparrow\downarrow})/2$, from which we can derive the singlet and the triplet excitation energies

$$\omega_{\mathrm{singlet}} = \omega_{12} + 2\Re \int \mathrm{d}^3 r \int \mathrm{d}^3 r' \varphi_1^*(\boldsymbol{r})\varphi_2(\boldsymbol{r}) \left[\frac{1}{|\boldsymbol{r}-\boldsymbol{r}'|} + f_{\mathrm{xc}}^{(1)}(\boldsymbol{r},\boldsymbol{r}',\omega)\right] \varphi_1(\boldsymbol{r}')\varphi_2^*(\boldsymbol{r}')$$

$$\omega_{\mathrm{triplet}} = \omega_{12} + 2\Re \int \mathrm{d}^3 r \int \mathrm{d}^3 r' \varphi_1^*(\boldsymbol{r})\varphi_2(\boldsymbol{r})\, f_{\mathrm{xc}}^{(2)}(\boldsymbol{r},\boldsymbol{r}',\omega)\varphi_1(\boldsymbol{r}')\varphi_2^*(\boldsymbol{r}'). \quad (47)$$

Several calculations for the lowest excitation energies of atoms and molecules have been performed with these formulas with very promising results (66,74,75). Further results on the SPA, including a discussion of why, and under which circumstances, the SPA is a good approximation, can be found in References 76 and 77.

It is also possible to derive an operator whose eigenvalues are the square of the true excitation energies, thereby reducing the dimension of the matrix equation (Equation 44) (78, 79). The starting point is the decomposition of the linear change of the density

$$\delta n_\sigma(\boldsymbol{r},\omega) = \sum_{ia} [\xi_{ia\sigma}(\omega)\varphi_{a\sigma}^*(\boldsymbol{r})\varphi_{i\sigma}(\boldsymbol{r}) + \xi_{ai\sigma}(\omega)\varphi_{a\sigma}(\boldsymbol{r})\varphi_{i\sigma}^*(\boldsymbol{r})], \quad (48)$$

where *i* denotes an occupied and *a* a virtual state. By inserting this expression in Equation 37, and after performing a series of algebraic manipulations, it is possible to prove that the poles of the response function can be determined as solutions of the non-Hermitian eigenvalue problem

$$\begin{pmatrix} \hat{L} & \hat{K} \\ \hat{K}^* & \hat{L}^* \end{pmatrix} \begin{pmatrix} \boldsymbol{X} \\ \boldsymbol{Y} \end{pmatrix} = \Omega \begin{pmatrix} -\hat{1} & \hat{0} \\ \hat{0} & \hat{1} \end{pmatrix} \begin{pmatrix} \boldsymbol{X} \\ \boldsymbol{Y} \end{pmatrix}, \quad (49)$$

where the operators are defined in the product space $\mathcal{S}_i \times \mathcal{S}_a$, where $\mathcal{S}_i$ and $\mathcal{S}_a$ are the space of occupied and virtual states, respectively. Furthermore, $\hat{L}$ has the definition

$$L_{ia\sigma,i'a'\sigma'} = \delta_{ii'}\delta_{aa'}\delta_{\sigma\sigma'}(\epsilon_{a\sigma} - \epsilon_{i\sigma}) + K_{ia\sigma,i'a'\sigma'}. \quad (50)$$

If the operators $\hat{L}$ and $\hat{M}$ are real (which is true if the Kohn-Sham orbitals and $f_{\mathrm{xc}}(\omega)$ are real-valued), the previous equation can be cast into the pseudoeigenvalue problem

$$\sum_{a'i'\sigma'} \left[\delta_{\sigma\sigma'}\delta_{aa'}\delta_{ii'}(\epsilon_{j\sigma} - \epsilon_{k\sigma})^2 + 2\sqrt{\epsilon_{a\sigma} - \epsilon_{i\sigma}} K_{ai\sigma,a'i'\sigma'}(\Omega) \sqrt{\epsilon_{a'\sigma'} - \epsilon_{i'\sigma'}}\right] \beta_{a'i'\sigma'}$$

$$= \Omega^2 \beta_{ai\sigma}. \quad (51)$$

The eigenvalues of this equation are the square of the excitation energies, whereas the eigenvectors can be used to calculate the oscillator strengths (78, 79).

## Some Results

FINITE SYSTEMS The first calculation of excitation energies within TDDFT was performed by Ando (22) to determine intersubband transitions in semiconductor heterostructures. Following this work, Zangwill & Soven (23) performed the first calculations for finite systems. Using the ALDA approximation to the xc kernel, they achieved a full self-consistent solution of Equation 38 in order to obtain the photoabsorption cross section of several rare gas atoms for energies just above the ionization threshold. Their calculation for Xe is reproduced in Figure 1, and illustrates the excellent agreement with experiment they obtained for the rare gases.

This good agreement with experiment is found not only in transitions to the continuum. In Table 1 the $^1S \rightarrow {}^1P$ excitation energies for several atoms are listed (66). The notation "LDA/ALDA" has the meaning that the ground state has been obtained with the LDA functional, whereas the calculation of the excitation energies was done with the ALDA. We use this notation consistently in the following. The first, perhaps surprising, fact is that the difference of Kohn-Sham eigenvalues is already quite close to the experimental excitation energies. Adding the TDDFT correction then brings the results very close to experiment. We furthermore notice that the EXX/PGG results are clearly superior to the LDA/ALDA. There are two fundamental approximations in these calculations: (*a*) To solve the linear-response



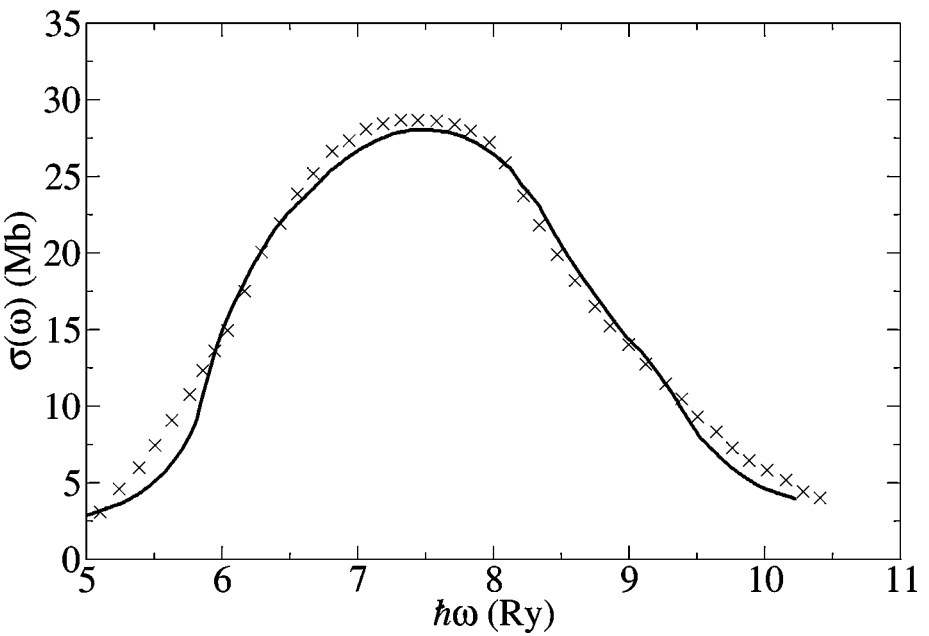


**Figure 1** Total photoabsorption cross section of xenon versus photon energy in the vicinity of the 4d threshold. The solid line is the TDDFT calculations of Zangwill & Soven (23) and the crosses are the experimental results of Haensel et al. (80).

**TABLE 1** $^1S \rightarrow {}^1P$ excitation energies for selected atoms. $\Omega_{exp}$ denotes the experimental results from Moore (81). All energies are in hartrees. Table adapted from Petersilka et al. (66)

| Atom | $\omega_{LDA}$ | $\Omega_{LDA/ALDA}$ | $\omega_{EXX}$ | $\Omega_{EXX/PGG}$ | $\Omega_{exp}$ |
|---|---|---|---|---|---|
| Be | 0.129 | 0.200 | 0.130 | 0.196 | 0.194 |
| Mg | 0.125 | 0.176 | 0.117 | 0.164 | 0.160 |
| Ca | 0.088 | 0.132 | 0.079 | 0.117 | 0.108 |
| Zn | 0.176 | 0.239 | 0.157 | 0.211 | 0.213 |
| Sr | 0.082 | 0.121 | 0.071 | 0.105 | 0.099 |
| Cd | 0.152 | 0.214 | 0.135 | 0.188 | 0.199 |



equation (Equation 38) we need the ground-state Kohn-Sham orbitals. These are normally obtained with an approximate ground-state xc potential. (*b*) Furthermore we have to approximate $f_{xc}$ (or the time-dependent $v_{xc}$). It turns out that the first approximation is much more important than the choice of $f_{xc}$ [this statement is in fact quite general for finite systems (62, 75)]. This is the reason for the superiority of the EXX/PGG results: As the EXX potential, in contrast to the LDA, exhibits the correct $1/r$ asymptotic behavior, it leads to much better unoccupied states, and consequently to better excitation energies.

TDDFT has also been applied to a variety of molecular systems, from small molecules (see e.g., References 73 and 82) to fullerenes (83–85) and even protein chromophores (64). The most commonly used approximation for $f_{xc}$ is the ALDA, but calculations have been reported using other functionals. The results are usually in very good agreement with experiment. In Figure 2 we show an example of an ALDA calculation, namely the absorption spectrum of the green fluorescent protein (GFP) (64). In nature, the chromophore of the GFP appears in two configurations, a neutral and an anionic configuration. The experimental spectrum includes contributions from both. From the figure it is clear that the positions of the peaks are in very good agreement with the measured spectra. Furthermore, by comparing the areas of the experimental and theoretical peaks we can estimate that the two forms of the photoreceptor appear in a $\sim$4:1 ratio, which is again in agreement with experimental findings.

Despite these unequivocal successes, there are finite systems for which the ALDA yields poorer results. For example, the ALDA sometimes underestimates the onset of absorption by 1 or 2 eV (62). However, this problem is solved by the use of functionals with the correct asymptotic behavior such as the EXX or the adiabatic LB94 (42). A more complicated problem is posed by the stretched $H_2$ molecule, where the ALDA fails to reproduce even qualitatively the shape of the potential curves for the $^3\Sigma_u^+$ and $^1\Sigma_u^+$ states (88, 89). A detailed analysis of the problem shows that the failure is related to the breakdown of the simple local approximation to the kernel.

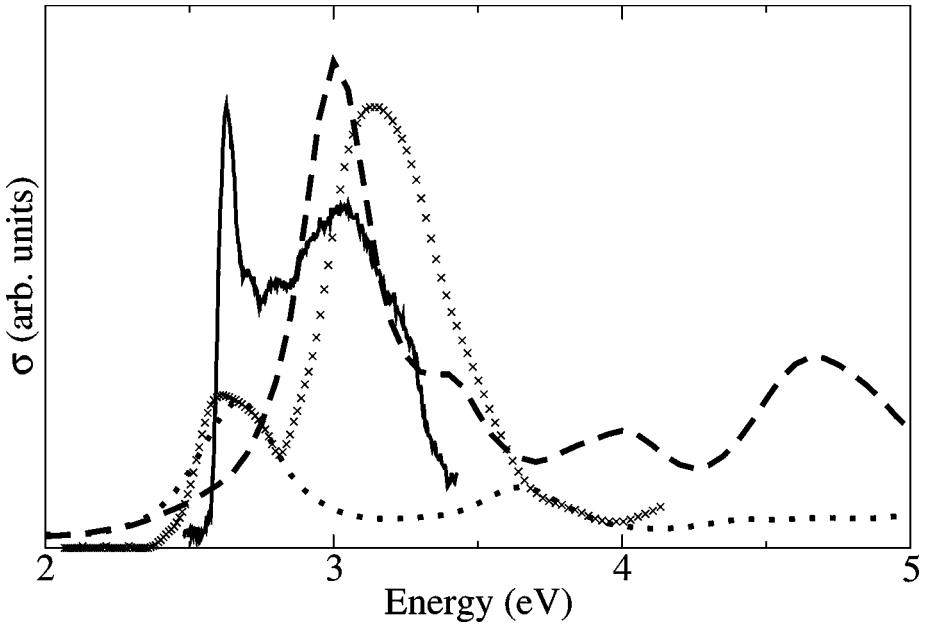


**Figure 2** The photoabsorption cross section of the chromophore of the green fluorescent protein calculated by Marques et al. (64) compared with the experimental measurements. The dashed line corresponds to the neutral chromphore, the dotted line to the anionic, whereas the crosses and solid curves are the experimental results of Nielsen et al. (86) and Creemers et al. (87), respectively.



EXTENDED SYSTEMS In a solid, the neutral excitations are related to the dielectric function that measures how the Coulomb interaction is screened by the electrons. For a spin-unpolarized system we can write the inverse dielectric function, $\varepsilon^{-1}$, in terms of the full density response function of the system, $\chi$. It reads

$$\varepsilon^{-1}(\boldsymbol{r}, \boldsymbol{r}', \omega) = \delta(\boldsymbol{r} - \boldsymbol{r}') + \int \mathrm{d}^3x \, \frac{\chi(\boldsymbol{x}, \boldsymbol{r}', \omega)}{|\boldsymbol{r} - \boldsymbol{x}|}. \tag{52}$$

To calculate the photoabsorption spectrum we have to look at the long-wavelength limit of Equation 52. The limit has, however, to be taken with care. We define the macroscopic dielectric function as

$$\varepsilon_{\mathrm{M}}(\omega) = \lim_{\boldsymbol{q}\to 0} \frac{1}{\varepsilon^{-1}(\boldsymbol{q}, \omega)_{\boldsymbol{G}=0,\boldsymbol{G}'=0}}, \tag{53}$$

where $\boldsymbol{q}$ is a vector of the first Brillouin zone, and $\boldsymbol{G}$ and $\boldsymbol{G}'$ are reciprocal lattice vectors. The photoabsorption spectrum can then be obtained from the imaginary part of the macroscopic dielectric function, $\sigma(\omega) = \Im\varepsilon_{\mathrm{M}}(\omega)$. Furthermore, the dielectric constant, $\varepsilon_0$, is the value of $\varepsilon_{\mathrm{M}}(\omega)$ at $\omega = 0$.

We have seen the excellent quality of the results obtained for finite systems using the ALDA. Naively we could perhaps expect that the same would occur for extended systems. This is unfortunately not the case.

An example where the ALDA fails is the calculation of nonlinear optical properties of long conjugated polymers (90, 91). Van Gisbergen et al. (90) found that the ALDA (as well as the adiabatic GGAs) overestimates hyperpolarizabilities by several orders of magnitude. The authors were able to trace back the problem to an incorrect electric field dependence of the xc potential: In a system with an applied electric field, the exact xc potential develops a linear part that counteracts the applied field (90, 92). This term is completely absent in both the LDA and the GGA, but is present in more nonlocal functionals like the EXX.

But perhaps the most spectacular failure of the ALDA is in the calculation of the photoabsorption spectrum of nonmetallic solids, especially in systems like wide band-gap semiconductors. If fact, the ALDA fails to give a significant correction to the simple RPA results. The reason is the following: For infinite systems, the Coulomb potential is (in momentum space) $4\pi/q^2$. It is clear from Equation 38 that if $f_{\mathrm{xc}}$ is to correct the RPA response for $q \to 0$, it will have to behave asymptotically like $1/q^2$ when $q \to 0$. This is not the case for the local or gradient-corrected approximations (they approach a finite value when $q \to 0$).

In Figure 3 we show the experimental photoabsorption spectrum of silicon (93) compared with several theoretical results. It is clear from the figure that the ALDA curve does not deviate much from the RPA results. Both underestimate the onset for absorption by around 0.5 eV, and fail to give the proper oscillator strength to the first peak. However, the spectrum obtained from the solution of the Bethe-Saltpeter equation (a many-body perturbational approach) is indeed very close to the experimental values. Several attempts have been made to correct this problem:

1. Using insight gained from the Bethe-Saltpeter equation, Reining et al. (72) proposed an $f_{\mathrm{xc}}$ of the form $-\alpha/q^2$ (the RORO kernel). By using the empirical value of $\alpha = 0.2$, they were able to describe quite well both the real and imaginary parts of the dielectric constant (see Figure 4). Unfortunately, the RORO kernel is semiphenomenological.
2. Kim & Görling (94) calculated the photoabsorption spectrum of silicon by using the EXX approximation both in the calculation of the ground state and for $f_{\mathrm{xc}}$. They found that the spectrum collapsed owing to the long-range nature of the Coulomb interaction. However, by cutting off the interaction, they were able to obtain results in very good agreement to the experimental curve.
3. In any finite system subject to an electric field, there is an accumulation of charge at the surface, which induces a counterfield inside the sample. In a solid, the problem is more complicated. As the solid is described by periodic boundary conditions, the density is the same in every unit cell. Clearly, it is not possible for any local (or semilocal) functional of the density to

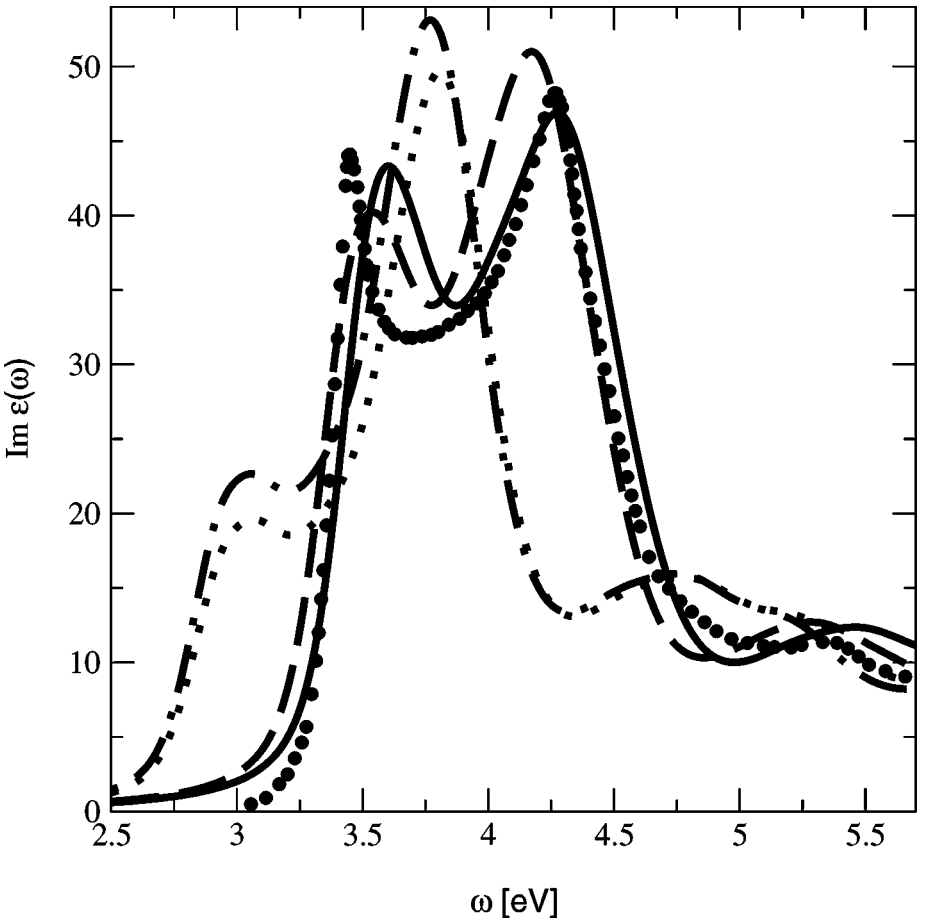


**Figure 3** Optical absorption spectrum of silicon. In the figure are represented the following spectra: experiment (93) (*thick dots*), RPA (*dotted curve*), TDDFT using the ALDA (*dot-dashed curve*), TDDFT using the RORO kernel (72) (*solid curve*), and the results obtained from the solution of Bethe-Saltpeter equation (*dashed curve*). Figure reproduced from Onida et al. (18).

describe the counter-field produced by the macroscopic polarization of the system (95–97). To circumvent this problem, Bertsch et al. (98) proposed to use as an extra dynamical variable the surface charge, or equivalently the macroscopic field produced by that charge. The whole scheme is especially well-suited to be used in a real-space, real-time approach (61, 99). Bertsch et al. did not calculate the spectrum of silicon, but their results for the simple metal lithium and for diamond are very encouraging (98).

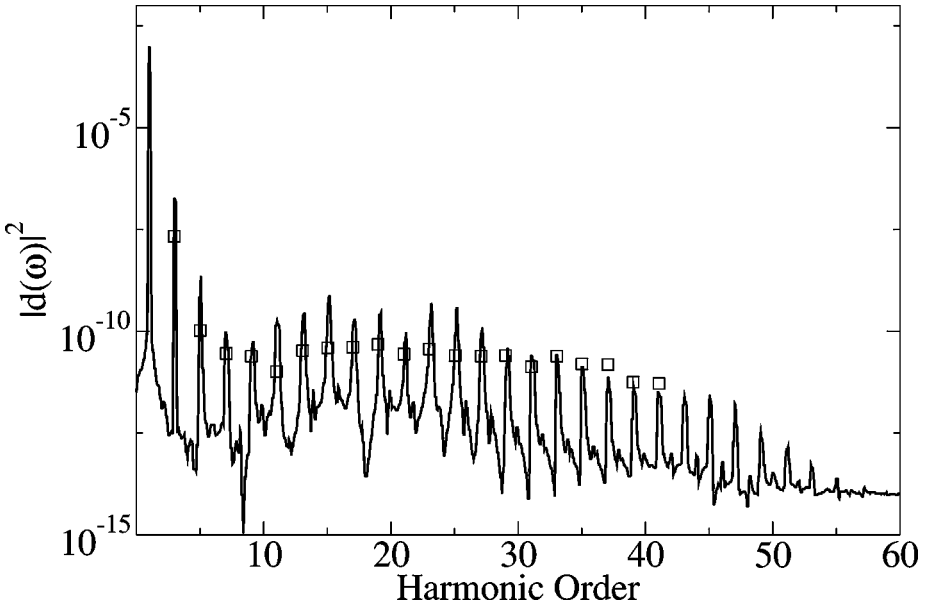


**Figure 4** Harmonic spectrum for He at $\lambda = 616$ nm and $I = 3.5 \times 10^{14}$ Wcm$^{-2}$. The squares represent experimental data taken from Miyazaki & Sakai (109) normalized to the value of the thirty-third harmonic of the calculated spectrum. Figure reproduced from Erhard & Gross (110).

4. Another way to take into account the macroscopic polarization is by using information coming from the current response of the system. Such an approach was followed by de Boeij et al. (100–102) that solved the response equations within a time-dependent current-density functional formalism, using a current-response kernel proposed by Vignale & Kohn in 1996 (103). Their calculations of the dielectric function for several semiconductors are in quite good agreement with experiment.

We remark that all these methods are the result of quite recent investigations, so it is very reasonable to expect further developments in the near future.

TDDFT can also be used to calculate the electron energy loss spectrum (EELS) of a system. The EELS is obtained from

$$\mathrm{EELS}(\boldsymbol{q}, \omega) = -\Im\left[\varepsilon^{-1}(\boldsymbol{q}, \omega)_{\boldsymbol{G}=0,\boldsymbol{G}'=0}\right], \tag{54}$$

Calculations of the EELS for silicon (18) and diamond (104) using the ALDA are in rather good agreement with experimental spectra, especially for small $\boldsymbol{q}$. These good results may come as a surprise in view of the failure of the ALDA to describe absorption spectra. However, it happens that for the calculation of the EELS

the most important ingredient is the proper inclusion of local field effects (i.e., the nondiagonal elements in $\boldsymbol{G}$ and $\boldsymbol{G}'$ of $\varepsilon$), while the choice of $f_{\rm xc}$ appears to be less important (104).

## NONLINEAR PHENOMENA

In this section we are concerned with problems where a linear-response description is not sufficient. Examples of such problems are the interaction of atoms or molecules with strong laser fields, or the scattering of a high energy projectile (like a proton) by a molecule. Clearly, to tackle this kind of problems within TDDFT, a full solution of the time-dependent Kohn-Sham equations (8) has to be performed.

### High-Harmonic Generation

If we shine a very intense laser field ($I > 10^{13}$ Wcm$^{-2}$) on an atom (or a molecule, or even a surface), an electron may absorb several photons and then return to its ground state by emitting a single photon. This photon has a frequency which is an integer multiple of the frequency of the external driving field. This process is called high-harmonic generation, and has received a great deal of attention from both theorists and experimentalists. As the outgoing photons maintain a fairly high coherence, high-harmonic generation can be used to build a source of coherent X-rays (105, 106).

TDDFT is a particularly adequate tool to study the interaction of matter with a strong laser field. We recall that from the time-dependent Kohn-Sham equations we can, in principle, obtain the exact density, $n(\boldsymbol{r}, t)$. Absorption and emission of light is determined by the time-dependent dipole moment of the system. For light polarized in the $z$ direction it reads

$$D(t) = \int \mathrm{d}^3 r\, z n(\boldsymbol{r}, t). \tag{55}$$

The absorption (or stimulated emission) spectrum is given essentially by the Fourier transform of $D(t)$ (107)

$$\sigma_{\rm absorption}(\omega) \propto \left| \int \mathrm{d}t e^{\mathrm{i}\omega t} D(t) \right|^2. \tag{56}$$

However, the spectrum of emitted radiation is approximately (i.e., neglecting incoherent processes) given by (107, 108)

$$\sigma_{\rm emission}(\omega) \propto \left| \int \mathrm{d}t e^{\mathrm{i}\omega t} \frac{\mathrm{d}^2}{\mathrm{d}t^2} D(t) \right|^2. \tag{57}$$

The dipole acceleration, $\mathrm{d}^2 D(t)/\mathrm{d}t^2$, can be obtained either by numerical differentiation, or by using Ehrenfest's theorem (108).

A typical high-harmonic spectrum is shown in Figure 4 for the He atom. The spectrum consists of a series of equispaced peaks at odd multiples of the external laser frequency (the even peaks are forbidden by inversion symmetry). The squares are at the experimental peak positions (109), and the solid line is the EXX/EXX calculation of Reference 110. The agreement is quite satisfactory. Furthermore, by using TDDFT, one can study the dependence of the harmonic spectrum on the driving laser. It was found that by changing the intensity or the spectral composition of the driving laser, the emission of harmonics can be enhanced sometimes by several orders of magnitude (110–112).



## Ionization Yields

In experiments employing low-intensity laser fields, electrons can only ionize if the frequency of the laser is larger than the ionization potential of the system. However, if the intensity of the laser is large enough, the electrons can ionize for any frequency of the applied laser through nonlinear processes. The measured energy spectrum of the outgoing photoelectrons is called the above threshold ionization (ATI) spectrum (113). An ATI spectrum typically consists of a sequence of equally spaced peaks at energies $E = (n + s)\omega - I_p$, where $n$ is a natural integer, $s$ is the minimum integer such that $s\omega - I_p > 0$, and $I_p$ denotes the ionization potential of the system.

A quantity related to the ionization probability is the number of charged atoms that leaves the interaction region. Figure 5 shows the yield of singly ionized and doubly ionized helium versus laser intensity (114). The solid curve on the right is the result of a calculation assuming a sequential mechanism for the double ionization of helium. Strikingly, this naïve sequential mechanism is wrong by six orders of magnitude for some intensities. This makes helium in a strong laser field one of the most correlated systems known in physics, and therefore, a very stringent test to TDDFT.

The Runge-Gross theorem tells us that the ionization yields are functionals of the time-dependent density. Unfortunately, and in contrast to the high-harmonic spectrum, we do not know how to write down these functionals exactly. Is is, however, possible to construct approximations to them by invoking a geometrical picture of ionization (115). Let us divide the three-dimensional space into a (large) box, $A$, containing the helium atom and its complement, $B$. Normalization of the many-body wave function then implies

$$1 = \int_A \int_A \mathrm{d}^3r_1\mathrm{d}^3r_2\,|\Psi(\boldsymbol{r}_1, \boldsymbol{r}_2, t)|^2 + 2\int_A \int_B \mathrm{d}^3r_1\mathrm{d}^3r_2\,|\Psi(\boldsymbol{r}_1, \boldsymbol{r}_2, t)|^2 + \int_B \int_B \mathrm{d}^3r_1\mathrm{d}^3r_2\,|\Psi(\boldsymbol{r}_1, \boldsymbol{r}_2, t)|^2\,, \tag{58}$$

where the subscript $A$ ($B$) means that the space integral is only over region $A$ ($B$). At sufficiently long time after the end of the laser pulse we expect all ionized electrons

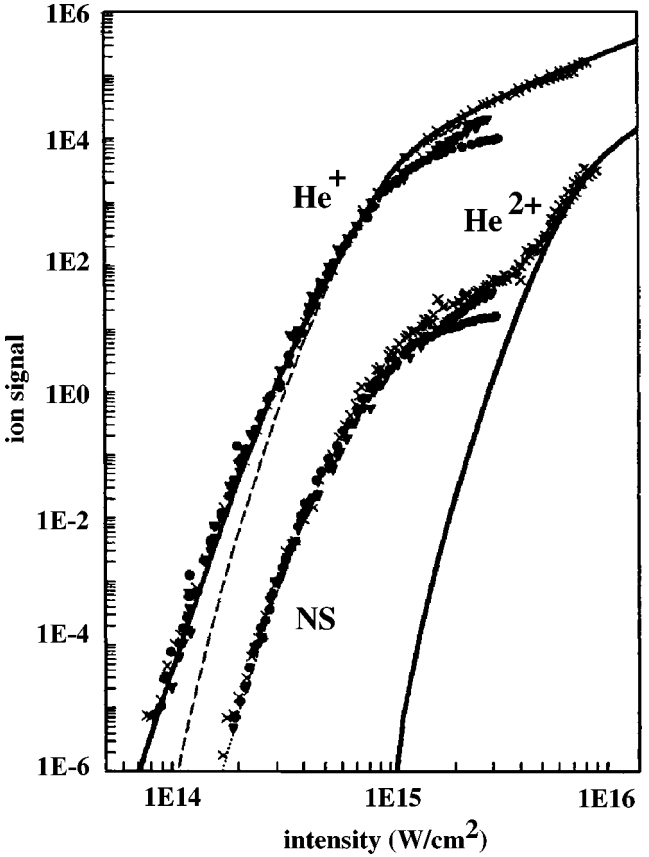


**Figure 5** Measured $He^+$ and $He^{2+}$ yields as a function of the laser intensity. The solid curve on the right is the $He^{2+}$ yield, calculated under the assumption of a sequential mechanism. Figure reproduced from Walker et al. (114).



to be in region *B*. Then the second term of Equation 58 can be interpreted as a single ionization probability, whereas the third measures the probability of double ionization. However, these terms are written in terms of the wave function and not of the density. To circumvent this problem we introduce the pair-correlation function

$$g[n](\boldsymbol{r}_1, \boldsymbol{r}_2, t) = \frac{2\,|\Psi(\boldsymbol{r}_1, \boldsymbol{r}_2, t)|^2}{n(\boldsymbol{r}_1, t)n(\boldsymbol{r}_2, t)}, \tag{59}$$

which can be approximated in terms of the density only. By taking the simplest approximation to the pair correlation function, i.e., $g[n] = 1/2$, Petersilka & Gross (115) calculated the ionization yields of helium. All xc functionals tested (ALDA, EXX, and SIC-LDA) clearly yielded a significant improvement over the sequential mechanism. However, TDDFT results are still wrong, sometimes by

two orders of magnitude, and fail to reproduce the characteristic knee in the double ionization curve (see Figure 4). Better functionals for $g[n]$ did not significantly improve the results. This may indicate that the crucial approximation is the one for $v_{\rm xc}[n]$. It was also found that the ALDA potential greatly overestimates the ionization yield. This is due to the incorrect asymptotic behavior of the ALDA potential: The electrons of helium are not sufficiently bound and ionize too easily.

## The Electron Localization Function



A large number of chemical and physical processes involve the dynamics of excited electrons. Some examples include the photoisomerization of retinal, the absorption and transfer of energy in chlorophyll, and the interaction of molecules with a strong laser. All these processes have something in common: There is a change in the bonding properties of the system. Clearly, to understand them, we would like to be able to visualize how the bonds were destroyed, created, or simply changed in character.

Unfortunately, it is very hard to visualize a chemical bond: The electronic density is usually a very smooth quantity, and does not easily reveal the subtleties of chemical bonding. However, one-electron orbitals stemming from a Hartree-Fock or a Kohn-Sham calculation extend over several atoms and do not represent a single bond. To overcome this problem Becke & Edgecombe (116) introduced the electron localization function (ELF). By looking at this function, it is a trivial matter to distinguish between simple, double, and triple bonds, and to recognize lone pairs (117). The ELF can also be used to rigorously classify chemical bonds (118).

The original derivation of the ELF was restricted to systems in their ground state, but recently Burnus et al. (T. Burnus, M.A.L. Marques & E.K.U. Gross, unpublished manuscript) extended this derivation to time-dependent systems. The basic ingredient entering the ELF is a function, $D_\sigma(\boldsymbol{r}, t)$, that measures the probability of finding an electron close, in space and time, to a reference electron of like spin. If the reference electron participates in a covalent bonding, and is therefore localized in the bonding region, this probability must be small. However, for a fully delocalized electron, this probability must be large. The function $D_\sigma(\boldsymbol{r}, t)$ is approximately given by

$$D_\sigma(\boldsymbol{r}, t) = \tau_\sigma(\boldsymbol{r}, t) - \frac{1}{4}\frac{[\nabla n_\sigma(\boldsymbol{r}, t)]^2}{n_\sigma(\boldsymbol{r}, t)} - \frac{j_\sigma^2(\boldsymbol{r}, t)}{n_\sigma(\boldsymbol{r}, t)}, \tag{60}$$

where $j$ is the absolute value of the current, and

$$\tau_\sigma(\boldsymbol{r}, t) = \sum_{i=1}^{N_\sigma} |\nabla \varphi_{i\sigma}(\boldsymbol{r}, t)|^2 \tag{61}$$

is the kinetic energy density. The function $D_\sigma$ is always $\geq 0$ but it is not bounded from above. We therefore define

$$\mathrm{ELF}(\boldsymbol{r},t)=\frac{1}{1+\left[D_\sigma(\boldsymbol{r},t)/D^0_\sigma(\boldsymbol{r},t)\right]^2}, \tag{62}$$

where $D^0_\sigma$ is a local density approximation to the function $D_\sigma$. With this definition, the ELF is dimensionless and lies between 0 and 1. Furthermore, a completely localized bond has ELF $\approx 1$, whereas for a delocalized electron gas ELF $\approx 1/2$.

To illustrate the usefulness of the time-dependent ELF in visualizing and interpreting complicated processes, Burnus et al. (T. Burnus, M.A.L. Marques & E.K.U. Gross, unpublished manuscript) performed TDLDA calculations of the excitation of acetylene by a moderately strong laser field, and of the scattering of a high-energy (yet nonrelativistic) proton by ethene. In the first case, the ELF clearly shows ionization of electrons in fairly localized packets, and the transition from the bonding $\pi$ to the antibonding $\pi^*$ state. In the latter simulation, the oscillation and breaking of bonds and the creation of lone pairs were clearly visualized.



## CONCLUSIONS

In this review we tried to give a fairly general overview of the work done in TDDFT since its foundations by Runge and Gross in 1984. Clearly, an enormous amount of progress has been made during the past 20 years—several fundamental problems were understood and some of them solved, a legion of new xc functionals were proposed (with varying degree of success), and the theory was applied to a vast number of problems in physics and chemistry. Probably, the major success of TDDFT is the calculation of linear excitation energies in finite systems: Even the simplest approximation to the xc potential, the so-called adiabatic LDA, yields remarkably good results. As a consequence, the linear-response TDDFT equations are by now implemented in every major quantum-chemistry code and are in extensive use by the community. Extended systems, such as polymers or bulk materials, pose a serious challenge. However, very recent developments in the field suggest that these systems also are well within the reach of the theory. In the nonlinear regime, TDDFT is by now able to describe harmonic generation and multiphoton ionization. TDDFT sometimes fails, such as in the description of the knee structure in the yield of doubly ionized helium or in the calculation of the excitation spectrum of dissociating $H_2$. These limitations require further research. Clearly, the quest for new, ever-better xc functionals is only beginning.

## ACKNOWLEDGMENTS

We would like to thank Nicole Helbig, Silvana Botti, and Patrick Rinke for their useful comments and suggestions during the preparation of the manuscript. Part of this work was supported by the EC RTN EXC!TiNG (HPRN-CT-2002-00317).

**The *Annual Review of Physical Chemistry* is online at http://physchem.annualreviews.org**

## LITERATURE CITED


1. Hohenberg P, Kohn W. 1964. *Phys. Rev. B* 136:864
2. Thomas LH. 1927. *Proc. Cambridge Philos. Soc.* 23:542
3. Fermi E. 1927. *Rend. Accad. Naz. Linzei* 6:602
4. Fermi E. 1928. *Z. Phys.* 48:73
5. Kohn W, Sham LJ. 1965. *Phys. Rev. A* 140:1133
6. Ceperley DM, Alder BJ. 1980. *Phys. Rev. Lett.* 45:566
7. Parr RG, Yang W. 1989. *Density-Functional Theory of Atoms and Molecules*. New York: Oxford Univ. Press
8. Dreizler RM, Gross EKU. 1990. *Density Functional Theory*. Berlin: Springer-Verlag
9. Fiolhais C, Nogueira F, Marques MAL, eds. 2003. *A Primer in Density Functional Theory. Lect. Notes Phys.*, Vol. 620. Berlin: Springer-Verlag
10. Mermin ND. 1965. *Phys. Rev. A* 137: 1441
11. Oliveira LN, Gross EKU, Kohn W. 1988. *Phys. Rev. Lett.* 60:2430
12. Kurth S, Marques M, Lüders M, Gross EKU. 1999. *Phys. Rev. Lett.* 83:2628
13. Rajagopal AK, Callaway J. 1973. *Phys. Rev. B* 7:1912
14. Dreizler RM, Engel E. 1998. In *Density Functionals: Theory and Applications*, ed. DP Joubert, pp. 147–89. Berlin: Springer-Verlag
15. Gross EKU, Kohn W. 1990. *Adv. Quantum Chem.* 21:255
16. Gross EKU, Dobson JF, Petersilka M. 1996. In *Topics in Current Chemistry*, ed. RF Nalewajski, 181:81. Heidelberg: Springer-Verlag
17. van Leeuwen R. 2001. *Int. J. Mod. Phys. B* 15:1969
18. Onida G, Reinig L, Rubio A. 2002. *Rev. Mod. Phys.* 74:601
19. Maitra NT, Burke K, Appel H, Gross EKU, van Leeuwen R. 2002. In *Reviews in Modern Quantum Chemistry: A Celebration of the Contributions of R. G. Parr*, ed. KD Sen, pp. 1186–225. Singapore: World Sci.
20. Marques MAL, Gross EKU. 2003. See Ref. 9, p. 144
21. Runge E, Gross EKU. 1984. *Phys. Rev. Lett.* 52:997
22. Ando T. 1977. *Z. Phys. B* 26:263
23. Zangwill A, Soven P. 1980. *Phys. Rev. A* 21:1561
24. Maitra NT, Burke K. 2001. *Phys. Rev. A* 63:042501

24a. Maitra NT, Burke K. 2001. *Phys. Rev. A* 64:039901

25. Maitra NT, Burke K, Woodward C. 2002. *Phys. Rev. Lett.* 89:023002
26. Levy M. 1982. *Phys. Rev. A* 26:1200
27. Levy EH. 1983. *Int. J. Quantum Chem. Symp.* 24:243
28. van Leeuwen R. 1999. *Phys. Rev. Lett.* 82:3863
29. Gross EKU, Ullrich CA, Gossman UJ. 1994. In *Density Functional Theory, NATO ASI Ser. B*, ed. EKU Gross, R Dreizler, 337:149–71. New York: Plenum
30. van Leeuwen R. 1998. *Phys. Rev. Lett.* 80:1280
31. Keldysh LV. 1965. *Sov. Phys. JETP* 20:1018
32. Liu K-L, Vosko SH. 1989. *Can. J. Phys.* 67:1015
33. Perdew JP, Burke K. 1996. *Int. J. Quantum Chem.* 57:309
34. Perdew JP, Kurth S, Zupan A, Blaha P. 1999. *Phys. Rev. Lett.* 82:2544; and references therein

34a. Perdew JP, Kurth S, Zupan A, Blaha P. 1999. *Phys. Rev. Lett.* 82:5179

35. Becke AD. 1983. *Int. J. Quantum Chem.* 23:1915
36. Becke AD. 1996. *J. Chem. Phys.* 104: 1040

37. Becke AD. 1998. *J. Chem. Phys.* 109: 2092
38. Sharp RT, Horton GK. 1953. *Phys. Rev.* 90:317
39. Grabo T, Kreibich T, Kurth S, Gross EKU. 2000. In *Strong Coulomb Correlations in Electronic Structure Calculations: Beyond the Local Density Approximation*, ed. VI Anisimov, pp. 203–311. Amsterdam: Gordon & Breach
40. Perdew JP, Zunger A. 1981. *Phys. Rev. B* 23:5048
41. Seidl M, Perdew JP, Kurth S. 2000. *Phys. Rev. Lett.* 84:5070
42. van Leeuwen R, Baerends EJ. 1994. *Phys. Rev. A* 49:2421
43. Ullrich CA, Gossmann U, Gross EKU. 1995. *Phys. Rev. Lett.* 74:872
44. Krieger JB, Li Y, Iafrate GJ. 1992. *Phys. Rev. A* 45:101
45. Dobson JF, Bünner MJ, Gross EKU. 1997. *Phys. Rev. Lett.* 79:1905
46. Almbladh C-O, von Barth U. 1985. *Phys. Rev. B* 31:3231
47. Gunnarsson O, Lundqvist BI. 1976. *Phys. Rev. B* 13:4274
48. Görling A. 1999. *Phys. Rev. A* 59:3359
49. Görling A. 2000. *Phys. Rev. Lett.* 85:4229
50. Perdew JP, Levy M. 1985. *Phys. Rev. B* 31:6264
51. Ziegler T, Rauk A, Baerends EJ. 1977. *Theor. Chim. Acta* 43:261
52. Theophilou A. 1979. *J. Phys. C* 12:5419
53. Gross EKU, Oliveira LN, Kohn W. 1988. *Phys. Rev. A* 37:2805
54. Gross EKU, Oliveira LN, Kohn W. 1988. *Phys. Rev. A* 37:2809
55. Oliveira LN, Gross EKU, Kohn W. 1988. *Phys. Rev. A* 37:2821
56. Nagy Á. 1998. *Phys. Rev. A* 57:1672
57. Andrejkovics I, Nagy Á. 1998. *Chem. Phys. Lett.* 296:489
58. Kohn W. 1986. *Phys. Rev. A* 34:737
59. Nagy Á. 1998. *Int. J. Quantum Chem.* 69: 247
60. Gidopoulos NI, Papaconstantinou PG, Gross EKU. 2002. *Phys. Rev. Lett.* 88: 033003
61. Yabana K, Bertsch GF. 1996. *Phys. Rev. B* 54:4484
62. Marques MAL, Castro A, Rubio A. 2001. *J. Chem. Phys.* 115:3006
63. Serra L, Rubio A. 1997. *Phys. Rev. Lett.* 78:1428
64. Marques MAL, López X, Varsano D, Castro A, Rubio A. 2003. *Phys. Rev. Lett.* 90: 258101
65. Gross EKU, Kohn W. 1985. *Phys. Rev. Lett.* 55:2850
66. Petersilka M, Gossmann UJ, Gross EKU. 1996. *Phys. Rev. Lett.* 76:1212
67. Petersilka M, Gossmann UJ, Gross EKU. 1998. In *Electronic Density Functional Theory: Recent Progress and New Directions*, ed. JF Dobson, G Vignale, MP Das, pp. 177–97. New York: Plenum
68. Richardson CF, Ashcroft NW. 1994. *Phys. Rev. B* 50:8170
69. Corradini M, del Sole R, Onida G, Palummo M. 1998. *Phys. Rev. B* 57:14569
70. Tokatly IV, Pankratov O. 2001. *Phys. Rev. Lett.* 86:2078
71. Burke K, Petersilka M, Gross EKU. 2002. In *Recent Advances in Density Functional Methods*, Vol. III, ed. V Varone, P Fantucci, A Bencini, pp. 67–79. Singapore: World Sci.
72. Reining L, Olevano V, Rubio A, Onida G. 2002. *Phys. Rev. Lett.* 88:066404
73. Grabo T, Petersilka M, Gross EKU. 2000. *J. Mol. Struct.* (*THEOCHEM*) 501: 353
74. March NH, Rubio A, Alonso JA. 1999. *J. Phys. B* 32:2173
75. Petersilka M, Gross EKU, Burke K. 2000. *Int. J. Quantum Chem.* 80:534
76. Gonze X, Scheffler M. 1999. *Phys. Rev. Lett.* 82:4416
77. Appel H, Gross EKU, Burke K. 2003. *Phys. Rev. Lett.* 90:043005
78. Casida M. 1996. In *Recent Developments and Applications in Density Functional Theory*, ed. JM Seminario, p. 391. Amsterdam: Elsevier
79. Bauernschmitt R, Ahlrichs R. 1996. *Chem. Phys. Lett.* 256:454

80. Haensel R, Keitel G, Schreiber P, Kunz C. 1969. *Phys. Rev.* 188:1375
81. Moore CE. 1971. *Natl. Stand. Ref. Data Ser.* 35, Vol. I–III. Washington, DC: US GPO
82. Vasiliev I, Öğüt S, Chelikowsky JR. 2002. *Phys. Rev. B* 65:115416
83. Yabana K, Bertsch GF. 1999. *Phys. Rev. A* 60:1271
84. Yabana K, Bertsch GF. 1999. *Int. J. Quantum Chem.* 75:55
85. Castro A, Marques MAL, Alonso JA, Bertsch GF, Yabana K, Rubio A. 2002. *J. Chem. Phys.* 116:1930
86. Nielsen SB, Lapierre A, Andersen JU, Pedersen UV, Tomita S, Andersen LH. 2001. *Phys. Rev. Lett.* 87:228102
87. Creemers TMH, Lock A, Subramaniam V, Jovin T, Völker S. 2000. *Proc. Natl. Acad. Sci. USA* 97:2974
88. Aryasetiawan F, Gunnarson O, Rubio A. 2002. *Europhys. Lett.* 57:683
89. Gritsenko OV, van Gisbergen SJA, Görling A, Baerends EJ. 2000. *J. Chem. Phys.* 113:8478
90. van Gisbergen SJA, Kootstra F, Schipper PRT, Gritsenko OV, Snijders JG, Baerends EJ. 1999. *Phys. Rev. Lett.* 83:694
91. Champagne B, Perpète EA, van Gisbergen SJA, Baerends EJ, Snijders JG, et al. 1998. *J. Chem. Phys.* 109:10489
92. Gritsenko OV, Baerends EJ. 2001. *Phys. Rev. A* 64:042506
93. Lautenschlager P, Garriga M, Viña L, Cardona M. 1987. *Phys. Rev. B* 36: 4821
94. Kim Y-H, Görling A. 2002. *Phys. Rev. Lett.* 89:096402
95. Resta R. 1994. *Rev. Mod. Phys.* 66:899
96. Gonze X, Ghosez P, Godby RW. 1995. *Phys. Rev. Lett.* 74:4035
97. Ortiz G, Souza I, Martin RM. 1998. *Phys. Rev. Lett.* 80:353
98. Bertsch GF, Iwata JI, Rubio A, Yabana K. 2000. *Phys. Rev. B* 62:7998
99. Vasiliev I, Öğüt S, Chelikowsky JR. 1999. *Phys. Rev. Lett.* 82:1919
100. de Boeij PL, Kootstra F, Berger JA, van Leeuwen R, Snijders JG. 2001. *J. Chem. Phys.* 115:1995
101. van Faassen M, de Boeij PL, van Leeuwen R, Berger JA, Snijders JG. 2002. *Phys. Rev. Lett.* 88:186401
102. van Faassen M, de Boeij PL, van Leeuwen R, Berger JA, Snijders JG. 2003. *J. Chem. Phys.* 108:1044
103. Vignale G, Kohn W. 1996. *Phys. Rev. Lett.* 77:2037
104. Waidmann S, Knupfer M, Arnold B, Fink J, Fleszar A, Hanke W. 2000. *Phys. Rev. B* 61:10149
105. Chang Z, Rundquist A, Wang H, Murnane MM, Kapteyn HC. 1997. *Phys. Rev. Lett.* 79:2967
106. Spielmann C, Burnett NH, Sartania S, Koppitsch R, Schnürer M, et al. 1997. *Science* 278:661
107. Sundaram B, Milonni PW. 1990. *Phys. Rev. A* 41:6571
108. Kreibich T, Lein M, Engel V, Gross EKU. 2001. *Phys. Rev. Lett.* 87:103901
109. Miyazaki K, Sakai H. 1992. *J. Phys. B* 25:L83
110. Ullrich CA, Erhard S, Gross EKU. 1996. In *Super Intense Laser Atom Physics* (*SILAP IV*), ed. HG Muller, MV Fedorov, pp. 267–84. Amsterdam: Kluwer
111. Erhard S, Gross EKU. 1997. In *Multiphoton Processes 1996*, ed. P Lambropoulos, H Walther, pp. 37–46. Bristol: IOP
112. Telnov DA, Wang J, Chu S. 1995. *Phys. Rev. A* 52:3988
113. Agostini P, Fabre F, Mainfray G, Petite G, Rahman NK. 1979. *Phys. Rev. Lett.* 42: 1127
114. Walker B, Sheehy B, Di Mauro LF, Agostini P, Schafer KJ, Kulander KC. 1994. *Phys. Rev. Lett.* 73:1227
115. Petersilka M, Gross EKU. 1999. *Laser Phys.* 9:105
116. Becke AD, Edgecombe KE. 1990. *J. Chem. Phys.* 92:5397
117. Savin A, Nesper R, Wengert S, Fässler TF. 1997. *Angew. Chem. Int. Ed. Engl.* 36:1808
118. Silvi B, Savin A. 1994. *Nature* 371:683

*Annual Review of Physical Chemistry*
*Volume 55, 2004*

# CONTENTS